

1 Use of poulticing in desalination of masonry units – implications on salt 2 deteriorated structures

3 *Swathy Manohar¹ and Manu Santhanam²*

4 *1 swathymanohar@yahoo.com*

5 *2 manus@iitm.ac.in*

6 Department of Civil Engineering, IIT Madras

7 8 **Abstract**

9 Cellulose poulticing is a widespread method of desalination in practice for removal of salts
10 from historic structures. Optimization of the process is essential, considering that
11 poulticing/desalination is the prime step during the protection of existing structures in the
12 coastal zone. Even though poulticing is widely used in European countries, it is not being
13 commonly applied in Indian structures, because the principle and efficacy of the method have
14 not been investigated so far for the masonry materials in the Indian historic structures with
15 specific microstructure. The current study investigates the effect of cellulose poulticing in
16 bricks considering the role of different pore sizes in the substrates and the removal of different
17 types of salts depending upon the pore distribution. The process was found around 74% more
18 efficient in removing Na_2SO_4 than NaCl , in materials with more micropores (pore size $< 1 \mu\text{m}$),
19 as demonstrated from scanning electron microscopy (SEM) images and analysis of pore
20 structure using mercury intrusion porosimetry (MIP) on brick samples. Interesting results on
21 the unsuitability of cellulose poulticing in certain materials and the reasons behind them were
22 obtained, which are based on the predominant transport mechanisms for salt removal. The
23 study would be a reference for initiating cellulose poulticing as a desalination method
24 effectively in the historic coastal structures of Southern India.

26 **Keywords:** Desalination, historic structures, protection, conservation, salt weathering

27 **Introduction**

28 Salt-induced degeneration is recognized as one of the most crucial causes of damage for
29 masonry structures¹⁻³. Salts introduced into the materials from external exposure can cause
30 crystallization inside the material microstructure owing to the changes in temperature, humidity
31 and depending upon the nature of salt. Repetitive dry-wet cycling increases the concentration
32 of salts inside the pores, causing them to get supersaturated and causing crystallization pressure
33 to the pore wall damaging the material. Hence, periodical removal of salts (desalination) is
34 essential from porous masonry to prevent deterioration, and is also a must pre-repair/protection
35 strategy while approaching salt-deteriorated structures with any kind of treatments.
36 Desalination techniques have not been explored significantly in India, despite the ease of
37 applicability and sustainable economic nature.

38 *Background*

39 Different desalination methods proposed/in use are broadly listed as diffusion (baths)⁴, electro-
40 migration, vacuum/water pressure extraction, using barium compounds to insolubilize the salts
41 by intervening at room temperature,⁵⁻⁷ and methods that use microbiological reaction or
42 microwave ovens⁸. Among these, immersion in water is a generally accepted method for
43 desalination in laboratory studies, but it is impractical for the existing structures. The use of
44 absorbent poultices is one of the most commonly used and an easily adaptable salt removal
45 technique for existing structures. Another solution to the problem of salt removal is the
46 application of products modifying crystallization kinetics. It is reported that such modifiers can
47 alter the supersaturation and permit migration of salts to the surface, by affecting the
48 evaporation rate⁹. For the transport of salts in very fine porous materials where other techniques
49 fail, electrochemical chloride extraction can be adopted. However, the electrical resistance of

50 the material and the varying tortuosity inside the pore system can adversely affect its efficiency,
51 by causing an inhomogeneous flow of current inside a highly layered and tortuous material
52 structure¹⁰.

53 Poulticing is considered as the most accepted method of salt removal from existing
54 structures^{11,12}. A better understanding of the process with various desalination methods would
55 provide guidelines for the engineers and conservators to efficiently select the poultice material
56 according to the existing exposure condition at the site and the substrate material. The efficacy
57 of the process depends on the transport phenomena in the material, which are indeed
58 determined by the pore structure and pore size distribution. The capillary suction provided by
59 the cellulose poultice to the substrate clearly depends on the size of pores in the substrate^{9,13}.

60 Nuclear Magnetic Resonance technology has been used in lab experiments to document the
61 performance of various poultices in contact with common substrates and has demonstrated that
62 the pore size of the substrate needs to be in proportion to that of the poultice for efficient
63 desalination¹⁴. Different poulticing materials that have been tested in the past are clays,
64 cellulose, minerals like diatomite, fume silica, rock wool and sacrificial mortars in the form of
65 lime - among which clays and cellulose are the most frequently used ones^{4,15,16}. Although clays
66 are appreciated for their good adhesion with the substrates, difficulty to cleanly remove them
67 makes their use restricted to objects without any heritage value¹⁷. Cellulose poulticing is
68 practised well in the western countries and has demonstrated effectiveness in removing
69 moisture as well as salt from structures, especially with high efficacy for brick masonry¹⁸.

70 Cellulose compounds are easy to work with, have a neutral pH, high plasticity and water
71 absorption, although the adhesiveness is poor (compared to clay) in vertical applications.
72 Hydrophilic mineral wool has been studied for its potential to be utilized for poulticing in
73 masonry materials as an alternative to cellulose, considering its advantages such as faster
74 transport of moisture and salt, repetitive usage etc.¹⁹ However, it could only be used for either

75 water transport (keeping the wool dry) or for salt transport (keeping the wool saturated) at a
76 time.

77 Optimizing the efficiency of poulticing in a particular material by designing the poultice with
78 new materials has been reported by Lubelli and Hees¹¹. Besides the pore structure of the
79 substrate, the mechanism of advection by the poultice can differ largely based on the kind of
80 salt to be removed. The mechanism of salt deposition and further crystallization differs for each
81 salt based on the chemical characteristics²⁰⁻²³. Kumar and Singh have reported the difficulties
82 faced in the removal of salts from the Mahabalipuram Shore Temple made of granite in Tamil
83 Nadu¹². Optimizing such situations requires experimental studies revealing the performance of
84 poulticing and its variation with respect to the controlling factors.

85 *Research significance*

86 The increasing risk of salt deterioration to historic structures due to the alarmingly changing
87 climatic conditions and floods has been reported worldwide²⁰. Even though flooding is a short-
88 term exposure of salt loads, the resulting dry-wet cycles in the affected structures stay active
89 for years and can even activate deep accumulated salts within the material from various past
90 sources. Recent studies from Europe show that desalination is the most suitable conservation
91 technique, among which poulticing is found as a promising and convenient method for the
92 immobile objects – related to heritage, including historic buildings. However, the transport
93 mechanisms in poulticing systems are not experimentally reported, which is crucial in
94 evaluating the effectiveness and performance of such methods. Despite its very common
95 application in architectural conservation, the method has produced questionable results with
96 different types of poultices, salts and substrates^{4,15}. No studies are reported to define the
97 variability in the efficiency of cellulose poulticing depending upon the combination of substrate
98 microstructure and type of salt. The present study addresses this issue, by experimentally

99 analysing the comparative efficacy of cellulose poulticing in masonry and correlating them to
100 the possible transport mechanisms through microanalytical techniques – using bricks of
101 different microstructures, exposed to different salts.

102 The current study investigates the effect of cellulose poulticing in bricks considering the factors
103 of different pore sizes in substrates and removal of different salts. Sodium sulphate and sodium
104 chloride are the salts considered in the study. Sodium sulphate is the most deleterious salt
105 causing degeneration in masonry materials, especially in materials with pores less than 1
106 $\mu\text{m}^{23,25}$. Sodium chloride was studied, considering the fact the most of the affected structures
107 in India lie in the coastal zone where sodium chloride is the major prevailing salt, even though
108 the damage of sodium chloride to the material is much lower compared to that of sodium
109 sulphate, with respect to salt crystallization²⁴.

110

111 **Materials and Methods**

112 *Properties of samples used*

113 Since pore structure is a critical material property that affects the process of poultice
114 desalination, 2 types of fired clay bricks depending upon their difference in pore structure were
115 selected for the study, which are commercially available and sourced from Chennai, India. The
116 first type of brick sample was denoted as HP – which was a “high porosity” brick, with large
117 pores and low density. The second type was denoted in the study as LP – which represents
118 “low porosity” brick, with more micropores and high density. 40 mm cube specimens were
119 made out of both the brick types (by removing the external exposed surfaces with irregularities
120 from all sides), each with variants of uncoated and coated with 2 different types of protective
121 coatings – one was a silicone-based water repellent (SC), and the other was an acrylic-siloxane
122 based water repellent (AS); these were reported as having entirely different mechanisms of

123 actions in the previous work by the authors²³. The cubes were cut out of the whole bricks using
124 a diamond blade cutting machine, and by using water as a coolant to prevent any crack
125 formation during the process of cutting. The samples for the tests were thus denoted as HP,
126 HP-SC, HP-AS, LP, LP-SC and LP-AS, where SC and AC represent two different types of
127 water repellent coatings. 3 replicates of each variant of specimens were tested used for all the
128 tests. The physicochemical and pore structure characteristics of the two brick types HP and
129 LP are given in Table 1. Compressive strength was measured as per IS 3945 (Part 1):1992 for
130 the bricks at a loading rate of 140 kg/cm²/minute and water absorption was measured according
131 to IS 3945 (Part 2): 1992. UPV (Ultrasonic Pulse Velocity) test was done on whole bricks,
132 using direct transmission method, in accordance with IS 13311-1:1992. Each numerical value
133 in the table is an average of 3 tests on similar samples. Bulk density was measured by Helium
134 gas pycnometer, and porosity and critical pore size were measured by Mercury Intrusion
135 Porosimetry (MIP).

136 *Method of desalination*

137 Cellulose poulticing was used as the technique for desalination in the study. Cellulose powder
138 from Arbocel was used, which has a uniform pore size distribution around 10 µm (with a single
139 peak as critical pore diameter of 10 µm). Dry cellulose powder was mixed for 1 minute with
140 water in the ratio 1:6 (by weight) to form the cellulose pulp. The required water content to
141 provide the poultice with adequate workability depends on the nature and particle size of the
142 particular poultice material. Here, the poultice to water ratio was fixed by trial and error
143 method, with the aim of obtaining a consistency that allows the pulp to mix well, stick to
144 specimens and not flow. The wet poultice was then applied to the surface of the salt weathered
145 specimens with approximately 1 cm thickness on all sides and kept for drying at room
146 temperature (25 °C) for 2 weeks, with polyvinylidene fluoride film covering for the initial 5
147 days to prevent evaporation. The moisture penetration depth of the cellulose poultice was

148 determined at 24 hours on a separate set of specimens with application of poultice on a single
149 face and was found to vary from 3 to 4 cm. The specimens were conditioned by drying at 40 C
150 until reaching constant mass and then cooling to room temperature before applying the
151 poultice. The moisture penetration was measured using a vernier callipers from the wet depth
152 from surface at mid-length on breaking each sample into two. The maximum drying shrinkage
153 of the poultice was measured as 5%. The poultice was removed on complete drying. The
154 specimens were then washed in water and dried to get desalinated specimens which were later
155 analyzed with microstructural characterization techniques. The process of preparation and
156 application of cellulose poultice on specimens was as shown in Figure 1. The cellulose powder
157 as such is shown, followed by the mixing of cellulose powder with water to form the pulp
158 (poultice) and then the samples covered by the prepared poultice.

159 *Microanalytical characterization techniques*

160 An Emcrafts GENESIS 2100 SEM (Scanning Electron Microscopy) equipment was deployed
161 to visualize the effect of cellulose desalination in the brick samples. Fractured surfaces of the
162 samples of size 5-8 mm were glued to the metallic stubs with carbon tape and were sputter-
163 coated with gold before viewing in the SEM. Secondary electron (SE) detector was used to
164 obtain SE images which showed the morphological features of pores opening up during the
165 desalination process.

166 Mercury Intrusion Porosimetry (MIP) was used to investigate the total open porosity and pore
167 size distribution at a microstructural level for the samples before and after desalination. The
168 instrument calculates the amount of mercury intruded under incremental pressures. Since the
169 pressure is inversely proportional to the pore size, the pore structure features can thus be
170 obtained from this experiment. Samples were first conditioned by drying at 40 °C until the
171 mass remains constant. Samples were then prepared as 4 similar small cubical pieces of 3 mm

172 size approximately from each brick, with a total mass in the range of 0.5-0.8 g. Hence, for a
173 single test, the 4 brick pieces from the same brick are placed in the dilatometer so that the test
174 result considers the average value of them. Using multiple pieces for the same test also ensures
175 high exposed surface area and high accessibility for mercury intrusion. 140-440 Pascal
176 porosimeter instrument from Thermo Scientific was used, which can measure pore sizes
177 ranging from 100 μm to 3 nm, by increasing pressure from vacuum to 400 MPa. The mercury
178 contact angle was assumed as 130°.

179 **Results and discussions**

180 Samples were subjected to accelerated salt crystallization weathering according to RILEM Test
181 no. V 1.b, 1980 for 112 consecutive dry-wet cycles with both sodium sulphate and sodium
182 chloride salts separately. The details of the weathering test methodology followed are given in
183 Table 2. The different degree of damage and different amount of salts inside the samples were
184 because of the pore size distribution of each sample^{10,11}. Poulticing with cellulose pulp was
185 applied on all the weathered samples to remove the salts, and the effect of desalination was
186 examined using microanalytical tests like SEM (for qualitative and visual investigation) and
187 MIP (for quantitative analysis).

188 *Scanning Electron Microscopy*

189 The effect of desalination on weathered samples was examined by capturing SEM images on
190 samples before and after desalination. Cellulose poulticing was found effective in removing
191 salts from the pores, for both sodium sulphate and sodium chloride salts, which is illustrated in
192 the SEM images shown in Figure 2-4.

193 Figure 2 shows the interior of a weathered (with Na_2SO_4 exposure) LP-SC sample after
194 desalination (sample was taken at a depth of 3-5 mm from the surface). Larger pores that
195 opened up without any salts in them are observed in this figure – this is indicative of the

196 efficiency of cellulose poulticing in removing the sodium sulphate salts from the bricks. EDS
197 spectrum was collected at the open pore observed in the SEM image in Figure 2 and is shown
198 adjacently. It is seen that sulphur was not shown in the spectrum, which is indicative of the
199 absence of sodium sulphate in the pores. The poulticing was also applied in samples subjected
200 to NaCl weathering. Figure 3 shows the surface of a weathered sample (HP) with NaCl
201 exposure, before and after desalination. EDS spectrum of the whole area of the SEM image in
202 Figure 3b also shows the absence of NaCl in the surface from the mineral composition. The
203 weathered surface before desalination (Figure 3 a) clearly exhibited larger NaCl crystals,
204 almost completely covering the exposed area. The image of the sample surface after
205 desalination showed that the NaCl crystals were completely removed from the surface, and in
206 addition, new small pores were opened up from which salts would have possibly been removed.
207 Figure 4 shows SEM images taken on desalinated samples collected 3-5 mm deep from the
208 surface of a weathered uncoated LP sample (with NaCl). The large group of micropores
209 observed shows that NaCl could deposit in pores of such small sizes, and poulticing could
210 remove NaCl salts even from these small pores. However, SEM images are insufficient to
211 quantify the efficiency of salt removal fully.

212

213 *Porosity measurements*

214 From the assurance that cellulose poulticing practically works for both Na₂SO₄ and NaCl salts,
215 Mercury Intrusion Porosimetry was carried out in the desalinated samples to identify the actual
216 pore structure and pore distribution on weathering, excluding the effect of possible salt
217 deposition.

218 Total porosities were measured for each specimen - before weathering, after accelerated
219 weathering and after desalination of accelerated weathered specimens, using MIP on samples

220 collected from 20 mm from the surface. Porosity changes were calculated from the data from
221 MIP tests conducted on the same samples corresponding to the stages of 'before weathering,
222 after weathering and after desalination'. The porosity values were then compared for each type
223 of brick exposed to the various salt solutions (Na_2SO_4 and NaCl) to compare the efficiency of
224 cellulose poulticing to remove salts, as shown in Figure 5. Comparing the change in porosities
225 on desalination among sulphate weathered samples, and chloride weathered samples, a general
226 observation that can be made is that cellulose poulticing is evidently more efficient in removing
227 sodium sulphate salts than sodium chloride salts from the low porosity bricks. Due to the
228 greater occurrence of macropores in the case of HP samples, sodium sulphate salt
229 crystallization and deposition is not highly favoured. The reason is the dissolution-mediated
230 phase transformation of sodium sulphate to reach supersaturations in smaller pores. This
231 process occurs because of the transitions between the two significant stable phases of sodium
232 sulphate called thenardite (Na_2SO_4) and mirabilite ($\text{Na}_2\text{SO}_4 \cdot 10\text{H}_2\text{O}$). Thenardite to mirabilite
233 conversion occurs by process of dissolution and recrystallization. As the relative humidity
234 decreases and evaporation rate increases, an increase in the relative proportion of thenardite is
235 observed. At equilibrium, thenardite is not expected to crystallize at temperatures less than 32.4
236 °C, but it occurs only at non-equilibrium condition in most porous materials. Below 32.4 °C,
237 mirabilite ($\text{Na}_2\text{SO}_4 \cdot 10\text{H}_2\text{O}$) is the stable phase. Mirabilite rapidly dehydrates at a relative
238 humidity (RH) below 71% (20 °C) to form thenardite. Thenardite will rehydrate to mirabilite
239 when the humidity exceeds 71%. So, a solution that is unsaturated with respect to thenardite
240 may already be highly supersaturated with respect to mirabilite. Figure 6 shows the X-ray
241 diffractograms of bricks affected by sodium sulphate (specimen LP is being shown) in which
242 simultaneous presence of mirabilite and thenardite can be seen. This discussion provides clarity
243 on the severity of damages associated with sodium sulphate salt. In the current case, this is
244 evident from the observation of the negligible difference in total porosity values before and

245 after desalination in HP, HP-SC and HP-AS samples as seen from Figure 5 (a). LP, with its
246 inherent micropores and newly formed micro-fissures on weathering, facilitated easy
247 crystallization and precipitation of sodium sulphate salts, which were then removed on
248 desalination. Whereas, the difference between total porosities before and after desalination in
249 case of chloride affected samples are much higher (Figure 5 b). This is because NaCl salt does
250 not face phase transitions, but gets precipitated and deposited on evaporation. Hence, a
251 remarkable number of macropores in HP would get filled with NaCl salts. The accumulated
252 NaCl salts from HP were then removed on desalination resulting in an increase of up to 13%
253 total porosity.

254 In the case of LP, the exposure of sodium chloride solution resulted in the deposition
255 of NaCl crystals in the larger portion of micropores which are abundant in the LP system.
256 Smaller ionic size and easy mobility of NaCl aids its deposition in micropores. Much higher
257 capillary action is required to remove these salts from the micropores - which would result in
258 a decreased efficiency of desalination in LP bricks when affected with NaCl. No difference in
259 trend was observed in case of the samples applied with the water-repellents in all the cases and
260 the reason could be their sacrificial behaviour during the accelerated salt crystallization tests.

261 Figure 7 shows the differential intrusion curves for the samples at different conditions
262 using the corresponding data derived from MIP test. The peak of each differential intrusion
263 curve represents the critical pore size of the sample, which is the pore diameter corresponding
264 to the maximum mercury intrusion, or it is similar to the most common pore size in the material.
265 Figure 7 a shows the differential intrusion curves for the high porosity brick HP, where the
266 nomenclature for reading the plots is as follows: HP is the curve corresponding to unweathered
267 form of the HP sample, HP Cl is that for HP weathered with chloride salt, HP Cl-de is the
268 desalinated form of HP Cl. This follows similarly for the low porosity brick LP also, in Figure

269 7 b. The upward shift of curves in the pre-peak region denotes the salt deposition in the pores
270 of that regime. The reversal of this upward shift denotes the removal of salts from those pores.
271 It can be seen from Figure 7 a that the critical pore size does not significantly change in the
272 highly porous brick HP, before and after weathering or desalination. This is because of the
273 inherent high salt weathering resistance of the HP brick due to larger pores in which salt
274 damage is minimum. The salt deposition in the case of HP is evident with chloride and sulphate
275 salts inside the pores, along with the effective removal of those salts (dotted lines), because of
276 the ease of removal from the large pores. In the case of LP, the salt deposition is higher for
277 sodium chloride (which can be seen from the larger area under the curve prior to peak);
278 however, the corresponding salt removal is not very significant, because of the failure of
279 capillary suction to transport salts from such smaller size, when the pore sizes in the poultice
280 are larger than that of bricks. However, the removal of the precipitated sodium sulphate salts
281 can be found more prominent in the case of LP. This is because sodium sulphate gets deposited
282 in the larger pores in the brick matrix (larger than that of the pores in cellulose poultice). These
283 observations are in support of the inferences out of the quantitative porosity analysis.

284 Figure 8 shows a schematic representation of the matrix of HP and LP bricks with large
285 pores and micropores respectively, where selective deposition of sodium sulphate and sodium
286 chloride crystals is shown. The figures are not drawn to scale. Figures 8 a and 8 b illustrate the
287 sodium sulphate crystals being deposited in the large pores of HP and small pores of LP. In
288 HP, the crystals are not facing any growth restraint; they are in equilibrium and do not cause
289 any crystallization pressure on the pore walls. In LP, there are smaller pores of different size
290 ranges. Sodium sulphate crystallizes and creates crystallization pressure on pores of size
291 between 0.2 and 1 μm predominantly in such type of microporous brick material^{23,26}. Pores
292 smaller than 0.2 μm are difficult to access for sodium sulphate crystals to get precipitated. That
293 is the reason why, in Figure 8 b, pores smaller than 0.2 μm remain empty, but salt crystals are

294 seen in the other pores. Figure 8 c and 8 d show the cases of HP and LP with NaCl precipitation
295 in the pores. In Figure 8 d, because of the very small ionic size and high mobility associated
296 with NaCl, the salt can get precipitated even in pores of size $0.01 \mu\text{m}^{11,23}$. However, the
297 capillary force induced by the cellulose poultice due to the correlation between pore size
298 distribution of the bricks and cellulose facilitates only salt absorption from pores larger than a
299 particular size⁴. Hence, in Figure 8 d, NaCl crystals do not get removed from some of the pores
300 of LP which are much smaller than that of the ability of cellulose poultice, thus decreasing the
301 efficiency of the desalination process. This would be the possible reason for reduced
302 desalination efficiency in removing NaCl from microporous material (LP) observed in the
303 porosity quantification study presented in Figure 5 b.

304 The movement of salts can generally happen by the action of diffusion where the ions
305 move owing to the difference in concentrations gradients between nearby areas (with the
306 principle of Fick's laws), and advection where ions move in the direction of flow of water²⁷.
307 Diffusion is the more natural process which has been prominent in the case of the current study,
308 between cellulose poultice and the bricks considered here (LP and HP). Advection can be
309 predominant in case of poulticing, because of the moisture state and condition of substrate
310 involved in the process. During the drying phase, when water evaporates out, salt can move
311 along with the liquid and take advantage of the transport direction. Advection is a faster
312 process; however, poultices should be specially designed with smaller pore sizes than that of
313 substrate for facilitating the advective component¹¹. The current study suggests that normal
314 cellulose poulticing is not efficient in removing NaCl from the very small pores available in
315 microporous dense materials like the LP bricks here, so process of advection may be further
316 studied by adopting mix compositions for cellulose with materials such as sand, kaoline etc.
317 that forms a pore structure denser than that of LP. If the poultice has a capillary pressure greater
318 than that in the substrate, during the force of poultice drying, advection will govern to extract

319 salts^{14,28,29}. Even when the Washburn's equation establishing the indirect relationship between
320 pore size and the capillary force is valid, it is convenient that the pores in the poultice are not
321 extremely small which slows down the process of salt transport. Hence, the current paper
322 demonstrates the importance of choosing the cellulose poultice material based on the kind of
323 salt and pore structure of substrate unit.

324 Considering the convenience and ease of using the poulticing technique for
325 desalination, the results from the study can be used to optimize the choice of poulticing to any
326 construction material such as concrete or any kind of stone depending upon their pore structure
327 and the kind of salt to which the structure is exposed. The texture of different materials inside
328 the pores may have an influence on the capillary action, which is not investigated in this study.
329 Any masonry material with a microporous structure such as granite (normally with a critical
330 pore size around 0.01 μm) or concrete (concrete with normal OPC or with blended cements
331 typically has a critical pore size around 0.1 μm) can have NaCl deposition in the micropores if
332 exposed to salt. NaCl is difficult to be removed by cellulose poulticing from the very fine
333 micropores because of the high surface tension of the molecules and the necessity of very high
334 capillary force. Whereas, sulphate exposure can deposit salts only in the available larger pores,
335 which can be easily and effectively removed by cellulose poulticing. Hence the method is
336 recommended for desalination in such materials (microporous) only if the exposure is
337 predominantly to sodium sulphate - which is the most deleterious salt. However, in the case of
338 materials with a large proportion of pores of size greater than 1 μm such as volcanic rocks
339 (basalt, pumice stone), coral stones, perforated or air-entrained concrete etc., either chloride or
340 sulphate salts would be seen precipitated in the large pores, and these can be effectively
341 removed with cellulose poulticing technique. For the microporous materials such as granite or
342 microporous bricks in the coastal areas, this paper emphasises the need for future studies for

343 desalination on techniques like electromigration, or poulticing combined with
344 electromigration.

345

346 **Conclusions**

- 347 • SEM images showed that cellulose poulticing was found to be effective in removing
348 both sodium sulphate and sodium chloride salts from the surface of any material. The
349 requirement of capillary force by the poultice to deploy the suction of salts was found
350 relevant only to the interior of the material where salts deposit inside the pores.

- 351 • On comparing the efficacy quantitatively by evaluating the total porosity using MIP on
352 salt weathered samples before and after poulticing at the interior (depth of 20 mm from
353 the surface), it was found that the process of desalination was around 74% more
354 efficient in removing sodium sulphate salts than sodium chloride salts, in materials with
355 more micropores (pore size $< 1 \mu\text{m}$). This is applicable in the case of any material
356 irrespective of the chemical nature, like bricks, stones (e.g. granite), concrete or mortar
357 that satisfies the prescribed pore size ranges.

- 358 • If the material is mostly comprised of macropores (pore size $> 1 \mu\text{m}$), desalination by
359 cellulose poulticing is equally efficient to remove sulphate and chloride salts. This is
360 valid for materials such as coral stone, volcanic stones like basalt, laterite, lightweight
361 concrete etc.

- 362 • The study shows the inefficiency of cellulose poulticing for the complete removal of
363 NaCl salts from more microporous system, where other advanced methods like
364 advection by designing a poultice with finer pore system or electrokinetic desalination
365 with migration component may be adopted as per the necessity.

366

367 **Conflicts of interest**

368 None

369 **References**

- 370 1. Flatt, R. J., Caruso, F., Sanchez, A. M. A., and Scherer, G. W. (2014). Chemo-
371 mechanics of salt damage in stone. *Nature Communications*, Nature Publishing Group,
372 5, 1–5.
- 373 2. Scherer, G., W., (1999). Crystallization in pores. *Cement and Concrete Research*;
374 29:1347–58.
- 375 3. Flatt, R. J. (2002). Salt damage in porous materials: How high supersaturations are
376 generated. *Journal of Crystal Growth*, 242(3–4), 435–454.
- 377 4. Vergès-Belmin, V. and Siedel, H. (2005). Desalination of Masonries and Monumental
378 Sculptures by Poulticing: A Review. *Restoration of Buildings and Monuments*
379 (*Bauinstandsetzen und Baudenkmalpflege*), 11(6): 391–408.
- 380 5. Weber, J., (2004) Insolubilisation of sulfate salts by baryum hydroxides : principles and
381 experiences, *Insolubilisation des sulfates par les hydroxydes de baryum: principes et*
382 *expérimentations*, in *Enduits dégradés par les sels: pathologies et traitements*, Journée
383 technique internationale, Paris 2004. Dossier technique ICOMOS-France 6 (2004).
- 384 6. Laue, S. 1996. Climate Controlled Behaviour of Soluble Salts in the Crypt of St Maria
385 im Kapitol, Cologne. In: R. Pancella, ed. *Actes du congrès LCP 1995 Conservation et*
386 *restauration des biens culturels*, Montreux, 24–29 sept. 1995. Lausanne: l'Ecole
387 Polytechnique Fédérale de Lausanne, pp. 447–54.
- 388 7. Bollingtoft, P., and Larsen, K., P., (2003), The use of passive climate control to prevent
389 salt decay in Danish churches, in *Mauersalze und Architekturoberflächen*,

390 Tagungsbeiträge 2002, H. Leitner, S. Laue and H. Siedel, Editors, 90-93, Hochschule
391 für Bildende Künste, Dresden.

392 8. Ranalli, G., Chiavarini, M., Guidetti, V., Marsala, F., Matteini, M., Zanardini and
393 Sorlini, C.,(1996) The use of microorganisms for the removal of nitrates and organic
394 substances on artistic stoneworks, in: "Proceedings of the 8th International Congress
395 on Deterioration and Conservation of Stone, Berlin, Germany. Josef Riederer, editor,
396 Berlin, p. 1415-1420.

397 9. Rivas, T., E. Alvarez, E., Mosquera, M., J., Alejano, L., Taboada, J. (2010),
398 "Crystallization modifiers applied in granite desalination: The role of the stone pore
399 structure", Construction and Building Materials, 24, 766–776

400 10. Lisbeth, M., Ottosen, Iben, V., Christensen (2012), "Electrokinetic desalination of
401 sandstones for NaCl removal—Test of different clay poultices at the electrodes",
402 Electrochimica Acta, 86, 192–202.

403 11. Lubelli, B., Hees R., P., J.,(2010), "Desalination of masonry structures: Fine tuning of
404 pore size distribution of poultices to substrate properties", Journal of Cultural Heritage
405 ,11, 10–18

406 12. Kumar, S. V., and Singh, M. R.,(2019), Salt Weathering of 7th Century CE Granite
407 Monument of Shore Temple, Mahabalipuram – Scientific Investigation and
408 Conservation Strategy, Heritage, 2, 230-253.

409 13. Benavente, D., García del Cura, M., A., García-Ginea, J., Sánchez-Moral, S., Ordóñez,
410 S., (2004), "Role of pore structure in salt crystallization in unsaturated porous stone",
411 Journal of Crystal Growth, 260, 532–44.

412 14. Voronina, V., (2011) Salt extraction by poulticing: an NMR study, Ph.D. Thesis,
413 Eindhoven University of Technology, 2011.

- 414 15. Vergès-Belmin, V., and H. Siedel, H., (2005). Desalination of Masonries and
415 Monumental Sculptures by Poulticing: A Review. *Restoration of Buildings and*
416 *Monuments = Bauinstandsetzen und Baudenkmalpflege* 11:1–18.
- 417 16. Borrelli, E., (2005). Desalination systems: types, applications and efficacy. In *Sais*
418 *sol'veis em argamassas de edificios antigos: danos, processos e soluções: Lisboa,*
419 *LNEC, 14 e 15 de Fevereiro de 2005. Lisbon: Laboratorio Nacional de Engenharia*
420 *Civil.*
- 421 17. Bowley M., J., (1975), desalination of stone: a case study, *Building Research*
422 *Establishment, Garston* 46.
- 423 18. Lombardo, T., and Simon, S., (2004) Desalination by poulticing: laboratory study on
424 controlling parameters, in *Proceedings of the 10th International Congress on*
425 *Deterioration and Conservation of Stone, Stockholm, 323-330, ICOMOS Sweden,*
426 *Stockholm (2004).*
- 427 19. Michálek, P., Tydlitát, V., Jerman, M., Černý, R., (2007), Desalination of historical
428 masonry using hydrophilic mineral wool boards, *Computational Methods and*
429 *Experimental Measurements XIII, Vol 46, pp 377-385, ISSN 1743-355X, WIT Press.*
- 430 20. Doehne, E., Schiro, M., Roby, T., Chiari, G., Lambousy, G., and Knight, H. (2008).
431 Evaluation of poultice desalination process at Madame John's Legacy, New Orleans. In
432 *Proc. 11th Int. Cong. on Deterioration and Conservation of Stone, J. Lukaszewicz, and*
433 *P. Niemcewicz, eds. Torun; Nicolaus Copernicus University Press, pp. 857-864.*
- 434 21. Blaeuer Boehm, C. (2005). Quantitative salt analysis in conservation of buildings. In
435 *Restoration of buildings and monuments: an international journal = Bauinstandsetzen*
436 *und Baudenkmalpflege: eine internationale Zeitschrift, vol 11(6) pp. 409-418.*
- 437 22. Manohar, S., and Santhanam, M., (2018), “Salt crystallization in building materials in
438 the marine environment”, 3rd R. N. Raikar Memorial International Conference &

- 439 Gettu-Kodur International Symposium on Advances in Science and Technology of
440 Concrete, American Concrete Institute - India Chapter, Mumbai, India,.
- 441 23. Manohar, S., Santhanam, M., Chockalingam, N., (2019) “Performance and
442 microstructure of bricks with protective coatings subjected to salt weathering”,
443 Construction and Building Materials (Elsevier) - Impact factor 4.046, Volume 226:94–
444 105. <https://doi.org/10.1016/j.conbuildmat.2019.07.180>
- 445 24. Manohar, S., Bala, K., Santhanam, M., Menon, A. (2020), “Characteristics and
446 deterioration mechanisms in coral stones used in a historical monument in a saline
447 environment”, Construction and Building Materials (Elsevier), Volume 241, 118102,
448 ISSN 0950-0618.
- 449 25. Manohar, S., and Santhanam, M., (2020): Correlation between Physical-mineralogical
450 Properties and Weathering Resistance Using Characterisation Case Studies in Historic
451 Indian Bricks, International Journal of Architectural Heritage, DOI:
452 10.1080/15583058.2020.1833108
- 453 26. Manohar, S.,(2020) A study on characterization, deterioration mechanisms and
454 protection of bricks and stones in historic structures, Ph D dissertation, Indian Institute
455 of Technology Madras (IIT Madras), Chennai.
- 456 27. Kröner, S., Alcaide, B., M., and Mas-Barberà, X.,(2016) Influence of substrate pore
457 size distribution, poultice type, and application technique on the desalination of
458 medium-porous stones, Studies in Conservation, 61:5, 286-296, DOI:
459 10.1080/00393630.2015.1131942
- 460 28. Sawdy, A. 2003. The Role of Environmental Control for Reducing the Rate of Salt
461 Damage in Wall Paintings. In: R. Gowing & A. Heritage, eds. Conserving the Painted
462 Past: Developing Approaches to Wall Painting Conservation. London: James & James
463 and English Heritage, pp. 95–109.



464 29. Pel, L., Sawdy, A. & Voronina, V. 2010. Physical Principles and Efficiency of Salt
465 Extraction by Poulticing. *Journal of Cultural Heritage*, 11: 59–67.

466

467

468 **Tables**

469 Table 1. Physico-mechanical and pore structure properties of the samples

Characteristics	HP	LP
Dimensions (mm)	220x110x50	220x110x50
Image		
Compressive strength (MPa)	8.1	12.3
Bulk density (g/cc)	1.65	2.10
Water absorption (%)	18.4	10.3
UPV (m/s)	1400	1950
Porosity (% from MIP)	49	31
Critical pore size (μm from MIP)	11.1	6.1

470

471 Table 2. Particulars of the accelerated weathering test adopted

Solution concentration	For sulphate weathering test: 10% Na_2SO_4 anhydrate solution For chloride weathering test: 15.6% NaCl solution
Duration of 1 cycle	24 hours: 2 h immersion, 19 h drying at 60 °C, 3 h room cooling (~ 27 °C)
Sample size	40 mm cubes

472

473

474 **Figures Legend**

475 Figure 1. Steps followed in the process of poulticing (a) cellulose powder in the dry form (b)
476 mixing of cellulose powder with water to prepare the poultice (c) samples covered with the
477 cellulose poultice left for drying

478 Figure 2. Interior of weathered (with Na_2SO_4) LP-1 sample after desalination

479 Figure 3. Surface of weathered (with NaCl) uncoated HP sample before and after desalination

480 Figure 4. Interior of weathered (with NaCl) uncoated LP sample after desalination

481 Figure 5. Comparison of total porosity values before and after desalination on (a) Samples
482 weathered with sodium sulphate (b) Samples weathered with sodium chloride

483 Figure 6. X-ray diffractogram of sulphate weathered LP brick sample showing presence of
484 mirabilite and thenardite

485 Figure 7. Differential Intrusion Curves of samples at different conditions (a) For the high
486 porosity brick sample HP (b) For the low porosity brick sample LP

487 Figure 8. Schematic representation of matrix of different samples showing crystallization of
488 salts in corresponding pores. (a) Sodium sulphate deposition in HP (b) Sodium sulphate
489 deposition in LP (c) Sodium chloride deposition in HP (d) Sodium chloride deposition in LP

490

491 **Figures**

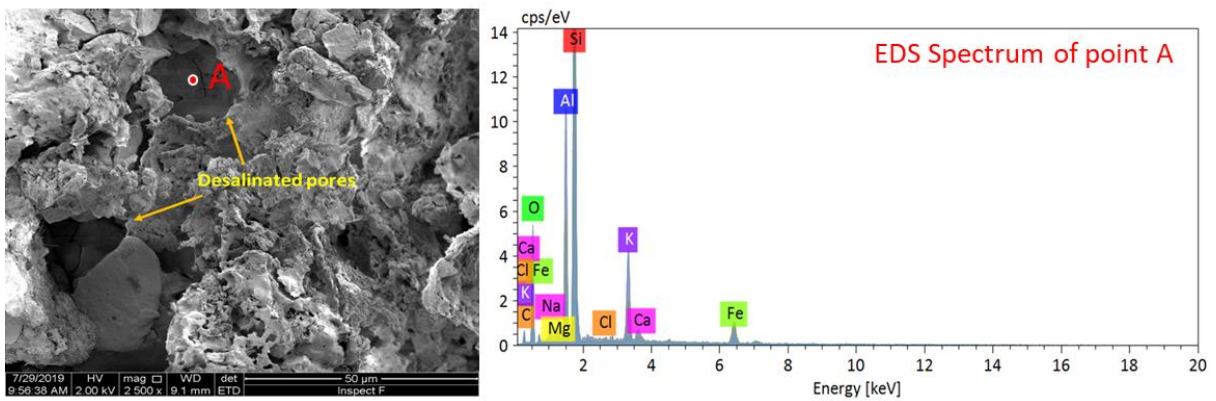
492



493

494 Figure 1. Steps followed in the process of poulting (a) cellulose powder in the dry form (b)
495 mixing of cellulose powder with water to prepare the poultrice (c) samples covered with the
496 cellulose poultrice left for drying

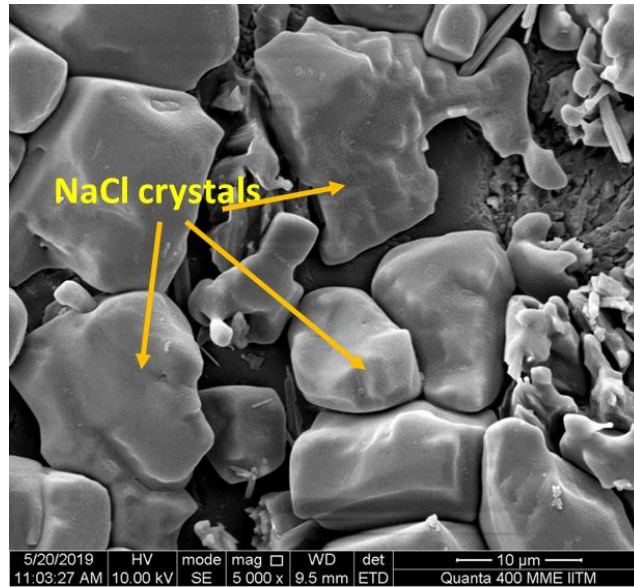
497



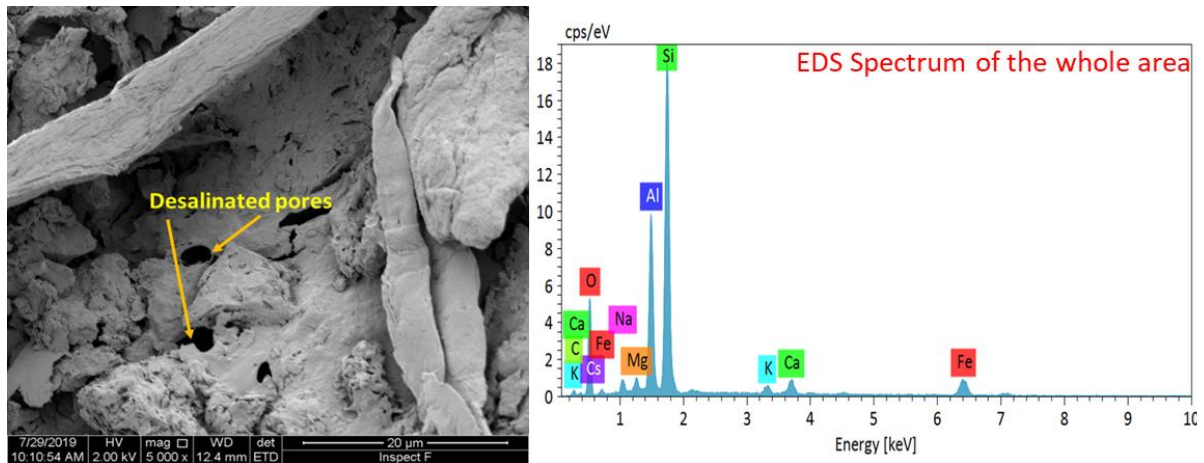
498

499 Figure 2. Interior of weathered (with Na_2SO_4) LP-SC sample after desalination, with the EDS

500

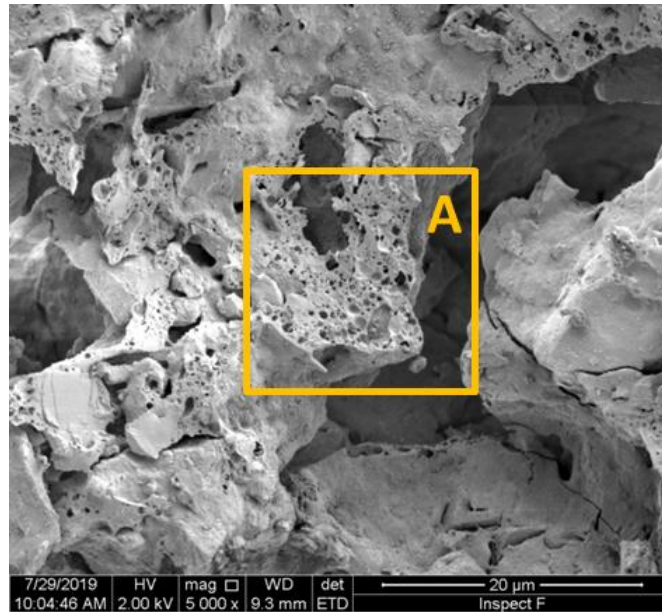


(a) Surface of a weathered uncoated HP sample showing NaCl crystals



(b) Surface of the sample after desalination showing pores opened-up, with the EDS spectrum

501 Figure 3. Surface of weathered (with NaCl) uncoated HP sample before and after desalination
 502



(a) Interior of the desalinated sample showing micropores

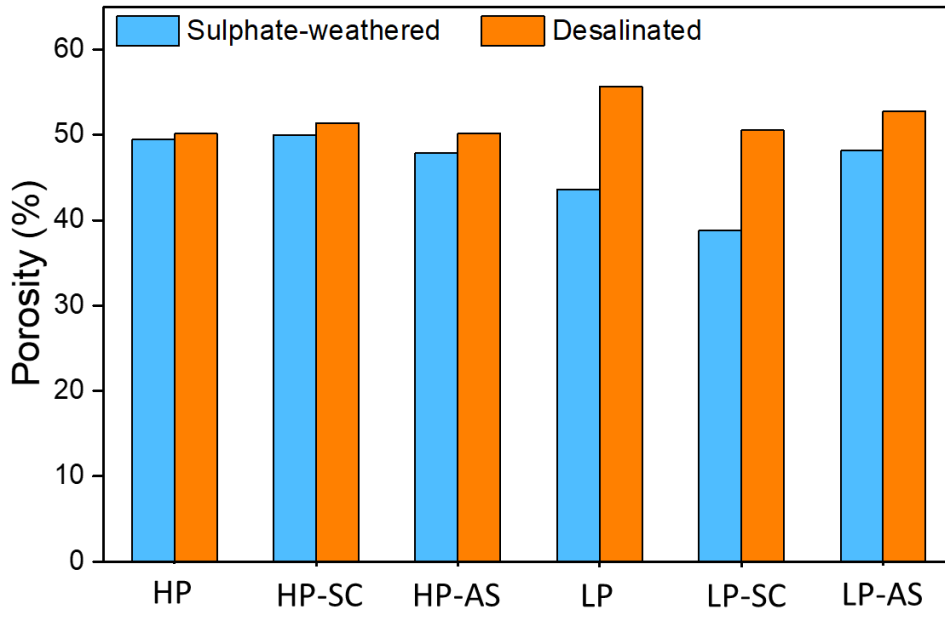


(b) Magnified view of 'A' marked in the previous figure

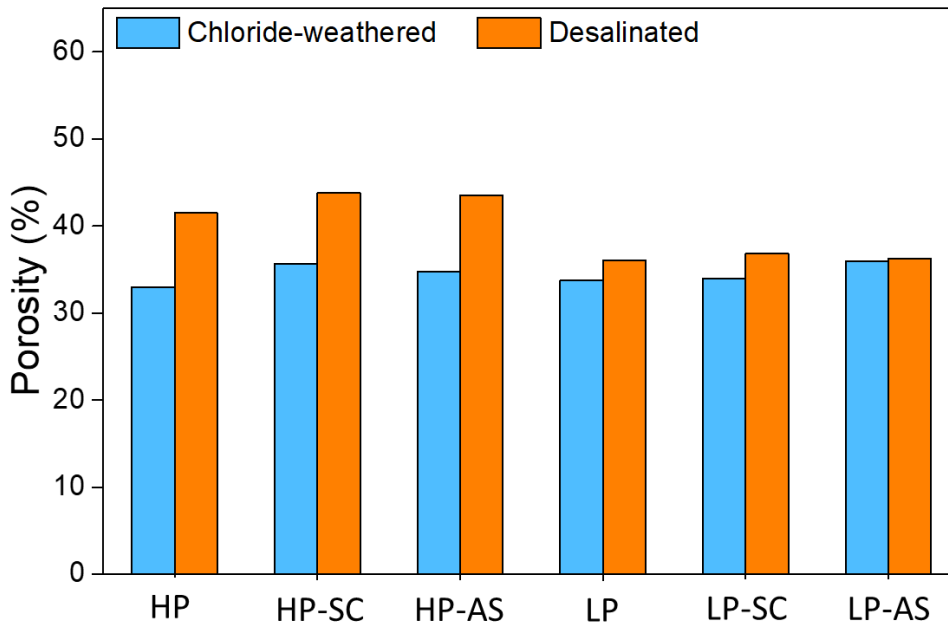
503

Figure 4. Interior of weathered (with NaCl) uncoated LP sample after desalination

504

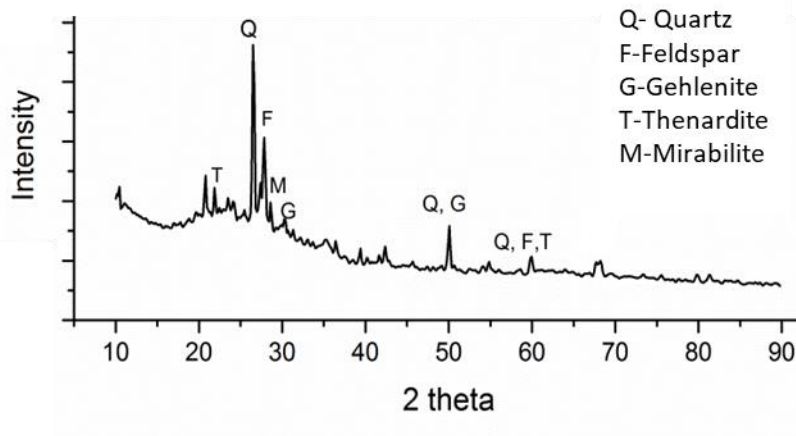


(a)



(b)

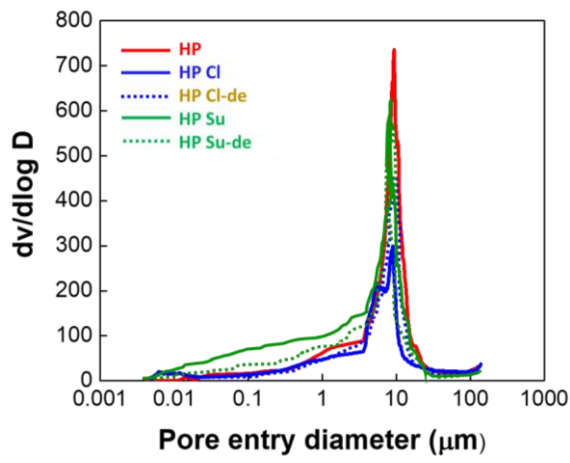
506 Figure 6. Comparison of total porosity values before and after desalination on (a) Samples
507 weathered with sodium sulphate (b) Samples weathered with sodium chloride



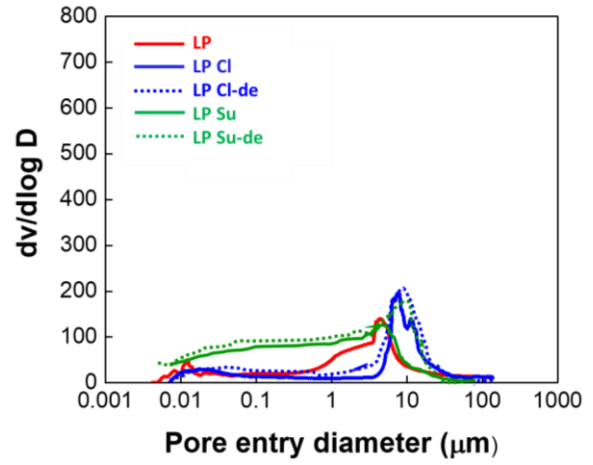
509

510 Figure 6. X-ray diffractogram of sulphate weathered LP brick sample showing presence of
511 mirabilite and thenardite

512



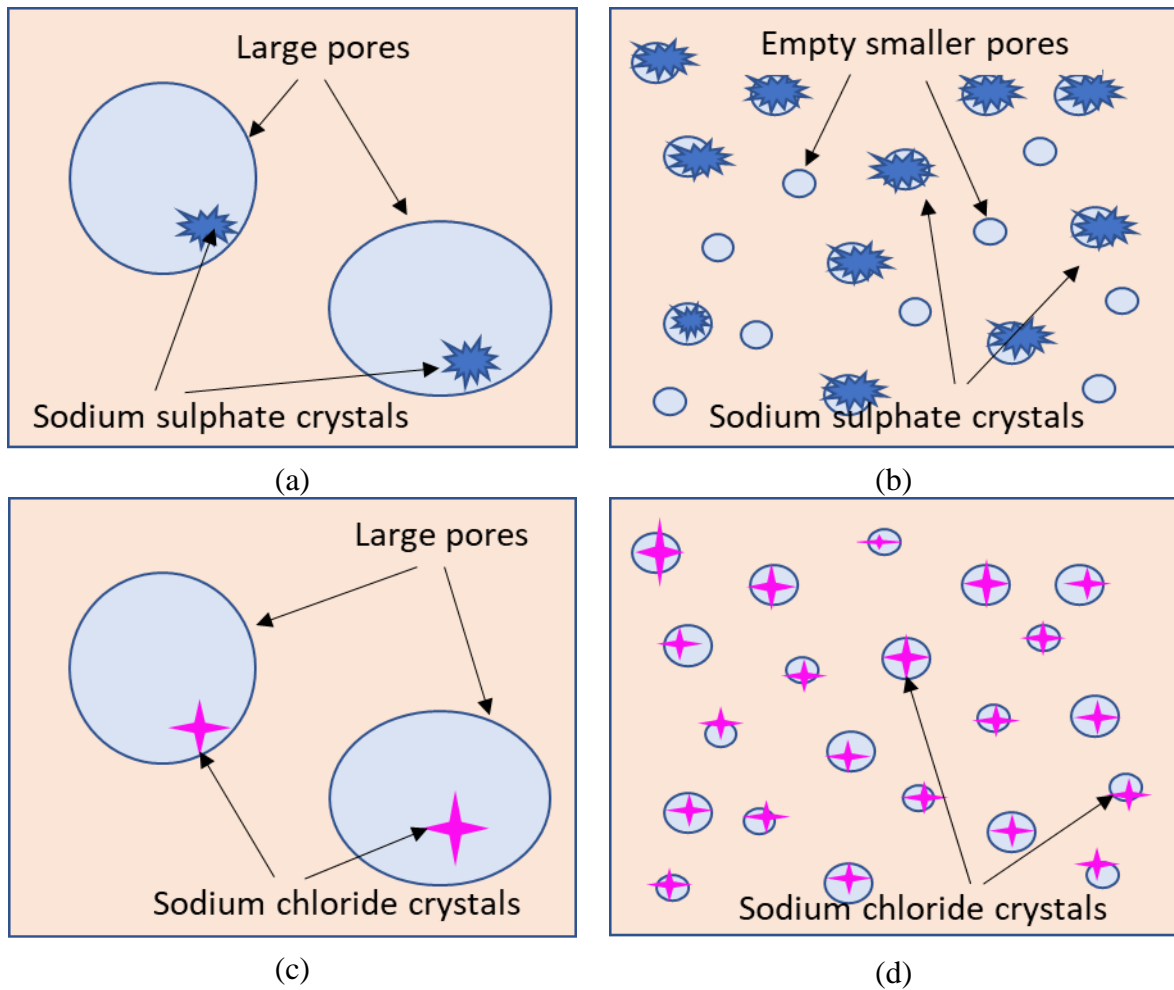
(a)



(b)

514 Figure 7. Differential Intrusion Curves of samples at different conditions (a) For the high

515 porosity brick sample HP (b) For the low porosity brick sample LP



517

518 Figure 8. Schematic representation of matrix of different samples showing crystallization of

519 salts in corresponding pores. (a) Sodium sulphate deposition in HP (b) Sodium sulphate

520 deposition in LP (c) Sodium chloride deposition in HP (d) Sodium chloride deposition in LP

521